Chapter 3

Magnetic Model

In this chapter, the micromagnetic model for the description of the magnetic properties of a laterally nanostructured film during growth is presented. The main physical idea of this model is to describe such a nanostructured system as an ensemble of interacting magnetic islands. The short-range exchange coupling, a uniaxial magnetocrystalline anisotropy, the long-range dipole coupling, and the coupling to an external field are taken into account within a Heisenberg-type model.

In **Sec. 3.1**, the magnetic interactions appearing in a Heisenberg-type spin model are introduced. **Sec. 3.2** summarizes previous results on the magnetization reversal of noninteracting single-domain islands due to an applied magnetic field and due to thermal activation. In addition, ensemble properties of such systems in thermodynamical equilibrium and nonequilibrium are discussed. In **Sec. 3.3**, the micromagnetic model suited for growing nanostructured films is presented. In **Sec. 3.4**, rates for magnetization reversals in interacting island systems are deduced. In addition to single-island flips, rates for coherent magnetization reversals of connected islands are treated. In Chapter 4, these flip rates will be applied to MC simulations of the magnetic ordering and relaxational behavior of ultrathin films during growth.

3.1 Magnetic interactions

For the description of the magnetism of a ultrathin film system, we start from a classical[1] Heisenberg model[2] with local anisotropy, long-range dipole

[1]For the length and time scales investigated in the present thesis, the neglect of the quantum nature of the magnetic moments is a satisfying approximation.

[2]The Heisenberg model with localized atomic magnetic moments $\boldsymbol{\mu}$ yields a good description of the magnetic properties of $4f$ metals. For itinerant magnetism - as present for the $3d$ metals Fe, Co, and Ni - the Heisenberg model still yields acceptable results. This is due to the fact that the spin density of the d electrons adopts large values only in a small

interaction, and an external magnetic field. The assumed model Hamiltonian reads

$$\mathcal{H} = \mathcal{H}_{\mathrm{ex}} + \mathcal{H}_{\mathrm{crys}} + \mathcal{H}_{\mathrm{dip}} + \mathcal{H}_{\mathrm{Z}} \quad . \tag{3.1}$$

The terms appearing on the right-hand side are explained below:

- The first term $\mathcal{H}_{\mathrm{ex}}$ describes the *short-range* Heisenberg *exchange* interaction. It results from the fact that for atoms with open electronic shells the Coulomb repulsion combined with the Pauli principle can lift the energetic degeneracy of the spin directions. In the Heisenberg model, the corresponding exchange energy term is written as [61]

$$\mathcal{H}_{\mathrm{ex}} = -\frac{1}{2} \sum_{i \neq j} J_{ij}\, \boldsymbol{s}_i\, \boldsymbol{s}_j \quad , \tag{3.2}$$

  where classical three-dimensional spins $\boldsymbol{s}_i = \boldsymbol{\mu}_i / \mu_i$ with unit length are assumed, representing the directions of the atomic magnetic moments $\boldsymbol{\mu}_i$. The exchange integral J_{ij} determines the relative spin directions. In the present thesis, only a uniform exchange integral $J_{ij} = J$ between nearest neighbors $\langle i, j \rangle$ is taken into account. Thus, the Heisenberg term simplifies to the *isotropic* expression

$$\mathcal{H}_{\mathrm{ex}} = -\frac{J}{2} \sum_{\langle i,j \rangle} \boldsymbol{s}_i\, \boldsymbol{s}_j \quad . \tag{3.3}$$

  For $J > 0$, the exchange interaction can lead to a spontaneous *ferromagnetic ordering* at temperatures below the Curie temperature T_{C}. The ferromagnetic ordering is characterized by a finite magnetization

$$\boldsymbol{M} = n \, \langle \boldsymbol{\mu} \rangle = n \, \mu_{\mathrm{at}} \langle \boldsymbol{s} \rangle \quad , \tag{3.4}$$

  where the brackets $\langle\ \rangle$ denote the expectation value in thermodynamical equilibrium and n is the spin density. For the description of real systems, J is treated as a parameter which can be adjusted to experimentally measured Curie temperatures $T_{\mathrm{C}} \approx qJ$, q being the coordination number. Thus, the order of magnitude results in $J \approx 10^2$ K $\approx 10^{-2}$ eV for bulk Fe, Co, and Ni.

- The second term $\mathcal{H}_{\mathrm{crys}}$ denotes the *magnetocrystalline anisotropy* which results from the on-site spin-orbit coupling and depends sensitively on the local electronic structure [164, 113]. A ferromagnetic system can minimize its magnetocrystalline anisotropy energy by aligning the magnetization along some preferred cystalline axes (easy axes). Generally,

range around the ion core, in contrast to the charge density [51].

the bulk and interface crystalline anisotropy can be expanded in successive powers of the direction cosines of the magnetization. For *uniaxial* systems, which will be investigated in this thesis, the corresponding Hamiltonian reads [23]

$$\mathcal{H}_{\text{crys}} = -K_{\text{crys}} \sum_i (s_i^\alpha)^2 \quad , \tag{3.5}$$

where $\alpha = x$ or z denotes the easy axis of the system, and where a positive anisotropy constant K_{crys} favors an alignment of the spins along the easy axis. For example, a uniaxial easy axis is present in crystals with hcp structure (e. g. bulk Co) along the c axis, or for surfaces or thin film layers perpendicular to the surface (out-of plane magnetization). For thin films, the crystalline anisotropy constant is typically of the order of $K_{\text{crys}} \approx 10^{-5} - 10^{-3}$ eV [23].

- The third term $\mathcal{H}_{\text{dip}}$ represents the *long-range* magnetostatic interaction between the magnetic moments of the atoms which is therefore also called *dipole* interaction. It results from the multipole expansion of the spin density distribution. This contribution can be written as [72, 23]

$$\mathcal{H}_{\text{dip}} = \frac{\mu_{\text{at}}^2}{2} \sum_{i \neq j} \frac{1}{r_{ij}^3} \left(\boldsymbol{s}_i \boldsymbol{s}_j - 3 \frac{(\boldsymbol{s}_i \boldsymbol{r}_{ij})(\boldsymbol{s}_j \boldsymbol{r}_{ij})}{r_{ij}^2} \right) \quad , \tag{3.6}$$

with μ_{at} being the atomic magnetic moment and $\boldsymbol{r}_{ij} = \boldsymbol{r}_j - \boldsymbol{r}_i$ the distance vector between the moments i and j. If all moments are assumed to be parallelly aligned, as a consequence of the dominating exchange interaction, the dipole energy may be rewritten as

$$\mathcal{H}_{\text{dip}} = \frac{\mu_{\text{at}}^2}{2} \sum_{i \neq j} \frac{s_i s_j}{r_{ij}^3} \left(1 - 3\cos^2\theta_{ij}\right) \quad , \tag{3.7}$$

where θ_{ij} is the angle between the magnetization $\boldsymbol{M}$ and the distance vector $\boldsymbol{r}_{ij}$. The dipole interaction is an *anisotropic* coupling and thus contributes to the total magnetic anisotropy. It is also called *shape anisotropy*, since due to the long-range property of this interaction the shape of a magnetic specimen is significant. The dipole interaction favors always a magnetization parallel to the surfaces of the magnetic system and thus preferres an in-plane magnetization for thin films. For a pair of next neighbored $3d$-atomic moments, the dipole energy is approximately 10^3-times smaller than the exchange energy and amounts to $\sim 10^{-5}$ eV.

- The last term $\mathcal{H}_{\mathrm{Z}}$ is the Zeeman term. It represents the coupling of the spins to an external magnetic field $\boldsymbol{B}$ and can be written as

$$\mathcal{H}_{\mathrm{Z}} = -\mu_{\mathrm{at}}\, \boldsymbol{B} \sum_i \boldsymbol{s}_i \quad . \tag{3.8}$$

For a $3d$-atomic moment and field $B = 1$ T, the order of magnitude for the Zeeman energy amounts to 10^{-4} eV.

Generally speaking, a finite-sized ferromagnetic system can minimize its total magnetic energy, Eq. (3.1), by the formation of *magnetic domains* with different magnetization directions and comparatively narrow *domain walls* in which the magnetization rotates continuously. This can be calculated by solving the Euler-Lagrange equation of the corresponding continuous variational problem, as shown e. g. in the textbook by Hubert and Schäfer [69]. For a system with uniaxial anisotropy the energy per spin of a 180° domain wall (Bloch wall) is given by

$$\gamma_{\mathrm{B}} = 4\sqrt{J\, K_{\mathrm{crys}} \,/\, 2} \quad , \tag{3.9}$$

which typically amounts to values of the order $10^{-3} - 10^{-2}$ eV. The width of the domain wall can be estimated by

$$\delta_{\mathrm{B}} = r_o\, \pi \sqrt{J \,/\, 2\, K_{\mathrm{crys}}} \quad , \tag{3.10}$$

where r_o is the interatomic distance. The overall magnetization of a ferromagnet with a multi-domain magnetic structure vanishes or is only very small. The spontaneous magnetization $\boldsymbol{M}$ is defined within a domain, where the magnetic moments are parallelly aligned due to the exchange interaction.

For small magnetic particles with extensions d less than the domain wall width δ_{B}, the single-domain state is energetically more favorable than the multi-domain state. Inserting typical bulk values for K and J into Eq. (3.10), we estimate the critical diameter of a single-domain particle to be $d_{\mathrm{c}} \approx \delta_{\mathrm{B}} \approx$ 10 nm. Thus, the ground state of small ferromagnetic islands of a growing thin film can assumed to be single-domain.

3.2 Single-domain magnetic islands

In this section, we discuss the magnetization reversal of a single-domain island due to (1) an applied magnetic field and (2) thermal activation. This section provides the physical foundation of our micromagnetic model for laterally nanostructured ultrathin films and of the island magnetization flip rates which will be applied in the MC simulations. Furthermore, the ensemble properties of *noninteracting* magnetic islands in thermodynamical equilibrium and nonequilibrium are discussed.

3.2.1 Magnetization reversal of an island

The first theoretical description of the magnetic switching of a small single-domain particle (of the order $d \lesssim 10$ nm) was given by Stoner and Wohlfarth [157, 158]. The authors assumed that due to the strong exchange coupling between the atomic spins, the particle is always in the single-domain state, in particular also *during* the magnetization reversal process. Thus, a magnetic particle containing N atomic magnetic moments $\boldsymbol{\mu}_{\mathrm{at}}$ can be described by a single giant moment $\boldsymbol{\mu} = N\boldsymbol{\mu}_{\mathrm{at}}$. This coherent rotation mode of the atomic magnetic moments was later called the Stoner-Wohlfarth (SW) model [110], which is a good approximation for small particles, see Appendix D.

Below, we discuss the magnetization reversal of a SW island, subject to an *effective* uniaxial anisotropy, resulting from the crystalline anisotropy, Eq. (3.5), and the shape anisotropy, Eq. (3.7), and exposed to an opposite external magnetic field, Eq. (3.8). The easy axis of the anisotropy defines the z axis of the coordinate system, the magnetic field $\boldsymbol{B} = B\hat{\boldsymbol{z}}$ is assumed to be collinear to the easy axis and aligned along the $-\hat{\boldsymbol{z}}$-direction, see Fig. 3.1.

From the Hamiltonian, Eq. (3.1), the magnetic energy $E(\phi)$ of the SW island as function of the angle ϕ between the magnetization direction and the $\hat{\boldsymbol{z}}$-direction is given by

$$\epsilon(\phi) = \frac{E(\phi)}{KN} = -\cos^2\phi - 2h\cos\phi \quad , \tag{3.11}$$

where we have introduced the reduced field $h = B\mu_{\mathrm{at}}/2K$, and where K is the effective anisotropy constant. In Fig. 3.2, a sketch of $\epsilon(\phi)$ is depicted as function of the angle ϕ for different strengths of the reduced field h. Depending on the applied field, the height of the energy barrier between the two minima varies; for fields $|h| \geq 1$ a maximum and a minimum are present.

After an analysis of Eq. (3.11) (using $\partial E/\partial\phi = 0$ and $\partial^2 E/\partial\phi^2 \lesseqgtr 0$), we distinguish two cases for the reversal process of the island magnetic moment from the initial state $\phi = 0$ to the reversed state $\phi = \pi$, and for the corresponding characteristic times τ, see Appendix D:

(1) For magnetic fields $|B| \geq |B_{\mathrm{c}}|$ ($|h| \geq 1$), the magnetic reversal from the maximum to the minimum of $E(\phi)$ is governed by *spin precession processes.* The order of magnitude of the switching time τ of the island moment is given by the spin precession time

$$\tau_{\mathrm{pr}} = \frac{2\pi\hbar}{\mu_{\mathrm{at}}\, B} \tag{3.12}$$

of a single *atomic* moment $\boldsymbol{\mu}_{\mathrm{at}}$ in the external magnetic field $\boldsymbol{B}$. Here, $\hbar = h/2\pi$ is Planck's constant.

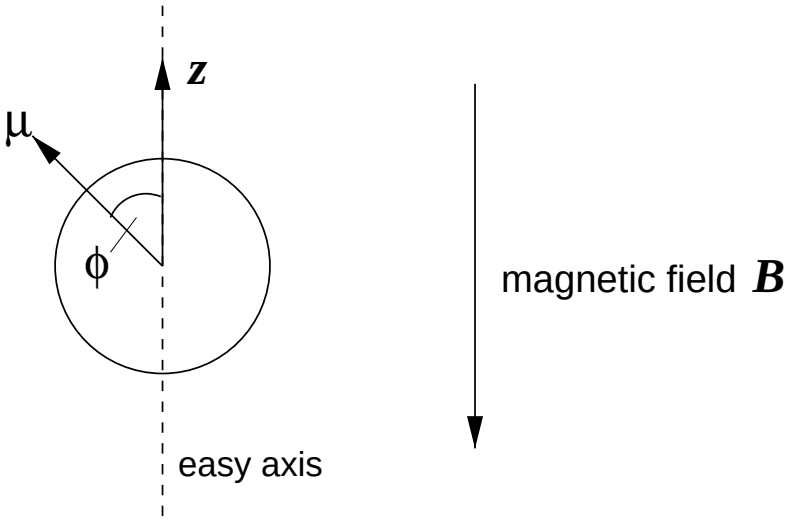

Figure 3.1: Sketch of a SW island subject to an opposite magnetic field $\boldsymbol{B} = B\hat{\boldsymbol{z}}$, $B < 0$. The z axis is the easy axis of the system, ϕ is the angle between the magnetic moment $\boldsymbol{\mu} = N\boldsymbol{\mu}_{\mathrm{at}}$ and the $+\hat{\boldsymbol{z}}$-direction.

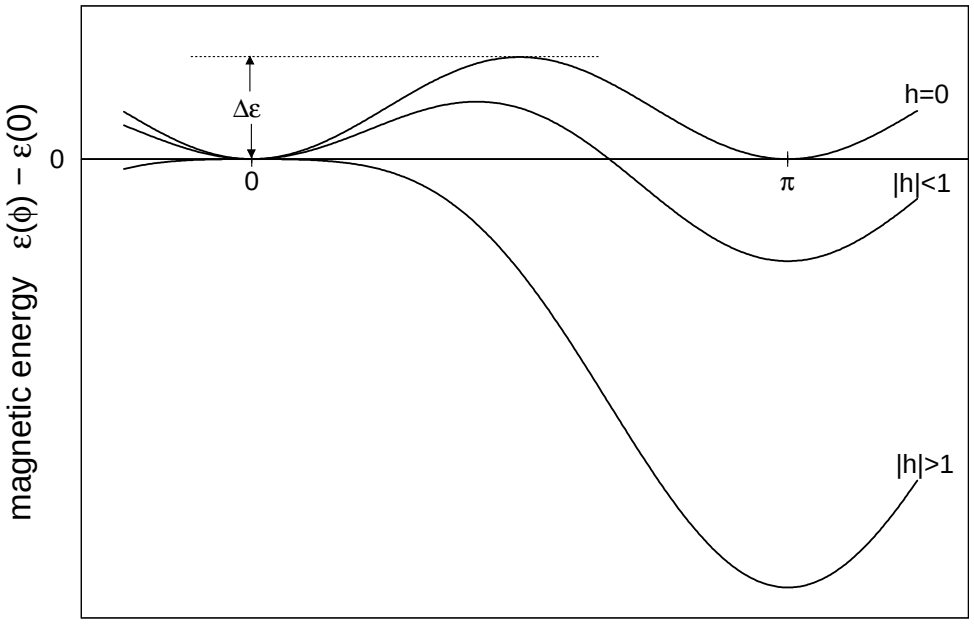

Figure 3.2: Sketch of the magnetic energy $\epsilon(\phi)$ of a SW island as function of the angle ϕ for different reduced fields h. The energy barrier $\Delta\epsilon = \Delta E/(KN)$ is indicated for the case $h = 0$.

(2) For $|B| < |B_c|$ ($|h| < 1$) a magnetization reversal over the anisotropy energy barrier

$$\Delta E = K\,N\,(1-h)^2 \quad . \tag{3.13}$$

can occur via *thermal activation*.[3] The order of magnitude of the characteristic time τ of such a process is given by the Néel-Brown model [112, 20, 21]

$$\tau = \tau_o \exp\left(\Delta E / k_B\,T\right) \quad , \tag{3.14}$$

where T is the temperature, k_B is Boltzmann's constant, and where τ_o is given by the spin precession time τ_{pr}^c of an atomic moment in the coercive field B_c (Eq. (3.12)), which typically amounts to $\tau_{pr}^c \approx 10^{-10} - 10^{-9}$ sec.

3.2.2 Noninteracting island ensembles

For magnetic fields $|B| \geq |B_c|$ the switching of island magnetic moments into the direction of the field evolves very fast, on a time scale of 10^{-10} sec. However, if energy barriers ΔE are present, then, the characteristic time τ for thermal switching depends exponentially on the ratio $\Delta E/k_B T$, according to the Néel-Brown model, Eq. (3.14). For an illustration the consequences of such a dependence, assume $\Delta E/k_B T \approx 25$, where an increase of this fraction by a factor 2 leads to 10^{11}-times larger τ! This has important implications for measurements on ferromagnetic particle systems.

Assume an ensemble of parallelly aligned, identical, *noninteracting* SW magnetic moments $\boldsymbol{\mu} = N\boldsymbol{\mu}_{at}$ with uniaxial anisotropy at time $t = 0$, at which an oppositely oriented magnetic field $\boldsymbol{B} = B\hat{\boldsymbol{z}}$ is applied. The total magnetization of the ensemble is measured after the time t_{exp}. On one hand, for switching times $\tau \gg t_{exp}$, the system remains in the nonequilibrium state, and a metastable ferromagnet close to its saturation magnetization $M_s = n\mu$ is observed, where n is the spin density. On the other hand, for $\tau \ll t_{exp}$, the thermodynamical equilibrium magnetization M_{eq} of the noninteracting system is measured, which amounts to $M_{eq} = 0$ for $B = 0$.

In the case of a vanishing anisotropy K, the equilibrium magnetization M_{eq}/n in direction of the applied field is given by the Langevin function [110]

$$\frac{\langle \mu^z \rangle}{\mu} = \mathcal{L}(y) = \coth y - \frac{1}{y} \quad , \tag{3.15}$$

where $y = \mu B/(k_B T)$.[4]

[3] Another possibility is quantum mechanical tunneling, as observed for molecular magnets [6].

[4] Wildpaner calculated the equilibrium magnetization M_{eq} of ensembles of small particles in external fields at finite temperatures using the MC technique. The author consid-

For a two-state model $\mu = \mu^z = \pm N\mu_{\mathrm{at}}$ (strong uniaxial anisotropy K), the equilibrium magnetization is given by the Brillouin function [110]

$$\frac{\langle \mu^z \rangle}{\mu} = \mathcal{B}(y) = \tanh y \quad . \tag{3.16}$$

In both cases, the system behaves like a paramagnetic ideal gas of noninteracting, giant magnetic moments $\boldsymbol{\mu} = N\boldsymbol{\mu}_{\mathrm{at}}$. This phenomenon is called *superparamagnetism* [110].

Roughly speaking, for given observation time t_{exp} the magnetization of the ensemble changes from the nonequilibrium to the superparamagnetic behavior at the so-called *blocking* temperature

$$T_{\mathrm{b}} = \frac{\Delta E}{k_{\mathrm{B}} \ln\left(t_{\mathrm{exp}}/\tau_o\right)} \quad , \tag{3.17}$$

which follows from Eq. (3.14).[5]

In the remainder of this section, we discuss the time dependence of the magnetic relaxation of a noninteracting island ensemble with uniaxial single-island anisotropies and parallel easy axes from a fully aligned state into thermal equilibrium $M_{\mathrm{eq}} = 0$. Assume the two-state model $\mu = \pm N\mu_{\mathrm{at}}$ for the directions of the island magnetic moments (strong uniaxial anisotropy). Then, in case of *identical* island sizes N, the relaxation of the magnetization of the system $M(t)$, after a saturating magnetic field has been switched off, is described by [110]

$$M(t) \propto \mu \, \exp\left(-2\,t/\tau\right) \quad , \tag{3.18}$$

where t is the time and where the characteristic time τ is given by the Néel-Brown model (Eq. (3.14)) and the anisotropy energy barrier $\Delta E = K\,N$. On the other hand, for *nonuniform* island sizes N_i, the decay of the magnetization of the ensemble follows a superposition of exponential laws, given by

$$M(t) \propto \sum_i \mu_i \, \exp\left(-2\,t/\tau_i\right) \quad , \tag{3.19}$$

where τ_i results from Eq. (3.14) and from the corresponding energy barrier $\Delta E_i = K_i\,N_i$ of island i.

---

ered exchange coupled *atomic* moments $\boldsymbol{\mu}_{\mathrm{at}}$. For spherical noninteracting identical particles with vanishing anisotropy, he found excellent agreement with the Langevin function $\mathcal{L}(y)$ and the SW model [174].

[5] Superparamagnetism is relevant for magnetic data storage devices, where bits must be stable for several years at room-temperature. For large storage densities, the bits must be as small as possible, but not smaller than the superparamagnetic limit, which therefore represents the natural limit for miniaturization [139].

3.3 Micromagnetic model of nanostructured films

In this section, the micromagnetic model for laterally nanostructured (island-type) films during growth is presented. It follows from a discretization of the nanostructured system by use of the SW model, and from the magnetic Hamiltonian, Eq. (3.1). The basic physical idea of this model is to describe a nanostructured film as a system of interacting, magnetic islands.

We treat each magnetic island i of a nanostructured film at coverage Θ and temperature T as a SW particle with single giant magnetic moment $\boldsymbol{\mu}_i = \mu_{\mathrm{at}}\, m_i\, N_i\, \boldsymbol{S}_i$. Here, $m_i(\Theta, T)$ is the coverage- and temperature-dependent relative *internal* island magnetization, $0 \leq m_i \leq 1$, due to the finite exchange coupling between the atomic magnetic moments and the finite size of the island. $N_i(\Theta)$ is the number of atoms of the island. The direction of the magnetic moment of the island is represented by the unit vector $\boldsymbol{S}_i = \boldsymbol{\mu}_i/\mu_i$.

The total (free) energy of this system of *interacting* magnetic islands is given by

$$E(\Theta, T) = E_{\mathrm{dw}}(\Theta, T) + E_{\mathrm{ani}}(\Theta, T) + E_{\mathrm{dip}}(\Theta, T) + E_{\mathrm{Z}}(\Theta, T) \quad . \tag{3.20}$$

The terms on the right-hand side are analogous to the terms of the Hamiltonian given by Eq. (3.1) and are explained in the following:

- The first term represents the inter-island exchange coupling or magnetic domain wall energy

$$E_{\mathrm{dw}}(\Theta, T) = -\frac{1}{2} \sum_{i>j} L_{ij}(\Theta)\, \gamma_{ij}(\Theta, T)\, \boldsymbol{S}_i \boldsymbol{S}_j \quad . \tag{3.21}$$

  If the magnetic moments of two *connected* islands i and j have opposite directions, they minimize their mutual exchange coupling by formation of a magnetic domain wall with energy $L_{ij}\gamma_{ij}$, where L_{ij} is the number of atomic bonds between the islands and γ_{ij} is the domain wall energy per atomic bond. The energy γ_{B} for an undisturbed Bloch domain wall in a bulk ferromagnet is given by Eq. (3.9). The corresponding energy of a domain wall with a finite extension in a nanostructured system is in general not known. Bruno recently studied constricted domain walls with atomic dimensions theoretically [24]. He showed that the wall width δ_{B} and the wall energy γ/J are independent of the material parameters and are determined only by the geometry of the constriction. Hence, in the present work, we treat γ_{ij} as a parameter and put $J > \gamma_{ij} > \gamma_{\mathrm{B}}$, as calculated in Ref. [24].

- The second term denotes the single-island effective uniaxial anisotropy energy

$$E_{\mathrm{ani}}(\Theta,T) = -\sum_i N_i(\Theta)\; K_i(\Theta,T)\; (S_i)^2 \tag{3.22}$$

with K_i the coverage- and temperature-dependent, effective anisotropy constant per atomic spin, which results from the magnetocrystalline anisotropy, Eq. (3.5), and the *intra*-island dipole coupling (shape anisotropy), Eq. (3.7). As an approximation, due to this anisotropy we allow only *two* stable directions for each island moment ($S_i = \pm 1$) along the easy axis. Two different geometries will be assumed: (1) an *out-of-plane* easy axis along the z axis ($S_i = S_i^z$) and (2) an *in-plane* easy axis along the x axis ($S_i = S_i^x$). We point out that a possible anisotropy energy barrier ΔE_i, Eq. (3.13), is still taken into account during magnetization reversal of an island.[6] In the case of an isolated island we obtain $\Delta E_i = N_i K_i$, which e. g. for $N_i = 10^3$ atoms is of the order $0.01 - 1$ eV.

- The third term describes the long-range *inter*-island dipole coupling between the magnetic moments $\boldsymbol{\mu_i}$

$$E_{\mathrm{dip}}(\Theta,T) = \sum_{i>j} \frac{\mu_i(\Theta,T)\,\mu_j(\Theta,T)}{r_{ij}^3}\left(\boldsymbol{S}_i\boldsymbol{S}_j - 3\,\frac{(\boldsymbol{S}_i\boldsymbol{r}_{ij})\,(\boldsymbol{S}_j\boldsymbol{r}_{ij})}{r_{ij}^2}\right), \tag{3.23}$$

where $r_{ij} = |\boldsymbol{r}_i - \boldsymbol{r}_j|$ is the distance between the centers of islands i and j. This dipole coupling is treated within the point-dipole approximation.[7] In the present thesis, the inter-island dipole energy is calculated by use of Ewald's summation technique for an infinite periodical arrangement of the unit cell *without* a cut-off radius. For this, we follow the description given by Jensen [76]; the application of his method is explained in detail in Appendix E. For an order-of-magnitude estimate of the dipole energy of an island pair, assume two near-neighbored *flat* islands, containing N_i atoms each. Then, the distance R between their centers is comparable to the diameters, $R \approx D \propto r_o\sqrt{N_i}$. The point-dipole energy of the island pair is $E_{\mathrm{dip}} \approx (N_i\,\mu_{\mathrm{at}})^2/R^3 \approx 5.37\cdot 10^{-5}\;(\mu_{\mathrm{at}}^2/r_o^3)\,\sqrt{N_i}$ [K]. For $\mu_{\mathrm{at}} = 2.0\,\mu_{\mathrm{B}}$, the atomic magnetic moment in units of Bohr magneton, measured for a 2-ML Co film [155], $r_o = 2.5$ Å the Co interatomic distance [124], and $N_i = 10^3$, one obtaines $E_{\mathrm{dip}} \approx 10^{-3}$ eV ≈ 10 K. Note that this

[6] Thus, the two-state approximation $S_i = \pm 1$ represents an Ising-type model including anisotropy energy barriers ΔE_i for the dynamics.

[7] The point-dipole approximation underestimates the exact dipole energy by maximally $\sim 50\%$ for closely neighbored islands, whereas it is already almost exact for island distances r_{ij}, larger than several times the island diameters [79].

value can be orders of magnitude larger than E_{dip} of a pair of next neighbored atomic moments.

- The last term describes the coupling of the island magnetic moments to an external magnetic field $\boldsymbol{B}$,

$$E_{\mathrm{Z}}(\Theta, T) = -\boldsymbol{B} \sum_i \mu_i(\Theta, T)\, \boldsymbol{S}_i \quad . \tag{3.24}$$

The *internal* magnetic order $m_i(\Theta, T)$ of a single island decreases for increasing temperature and depends on the finite size. This leads to varying effective single-island anisotropy coefficients $K_i(\Theta, T)$ and domain wall energies $\gamma_{ij}(\Theta, T)$. In the present thesis, these quantities are estimated within a mean-field theory (MFT) which is given in Appendix F.1.

We emphasize that Eq. (3.20) describes a system of separated dipole-coupled islands at coverages Θ far below the percolation threshold $\Theta \ll \Theta_{\mathrm{P}}$ (where $L_{ij} = 0$) as well as a connected ferromagnetic film at much larger coverages $\Theta \gg \Theta_{\mathrm{P}}$ (where $L_{ij} \gg 0$). We point out that the transition between these extremal cases during film growth is described within the same model.

Generally, such an interacting island ensemble represents a spin-glass-type system, characterized by *nonuniform* competing interactions [11]. The assumption of individual magnetic islands with varying sizes $N_i(\Theta)$ and bond lengths $L_{ij}(\Theta)$ – as resulting from the growth procedure, see Fig 2.8, p. 32 – is a natural discretization of the system. This is a good working hypothesis as long as the ultrathin film remains laterally nanostructured. However, for smooth (uniform) films the nonuniform quantities $N_i(\Theta)$ and $L_{ij}(\Theta)$ may represent an unphysical discretization of the system due to the artificially induced randomness.

Similar micromagnetic models have been reported in literature, on one hand for the description of continuous 2D systems [101, 88, 116], e. g. of thin polycrystalline MnBi films [118], and on the other hand for 2D or 3D systems of separated magnetic particles [9, 26, 57, 41]. So far, only few calculations have been performed on the basis of coverage- or particle-concentration-dependent models [62, 143, 121]. In many studies, not all interaction terms have been taken into account.

3.4 Island magnetization flips in the effective field

In this section, rates for island magnetization reversals of *interacting* islands – as described by the micromagnetic model, Eq. (3.20) – are deduced. In

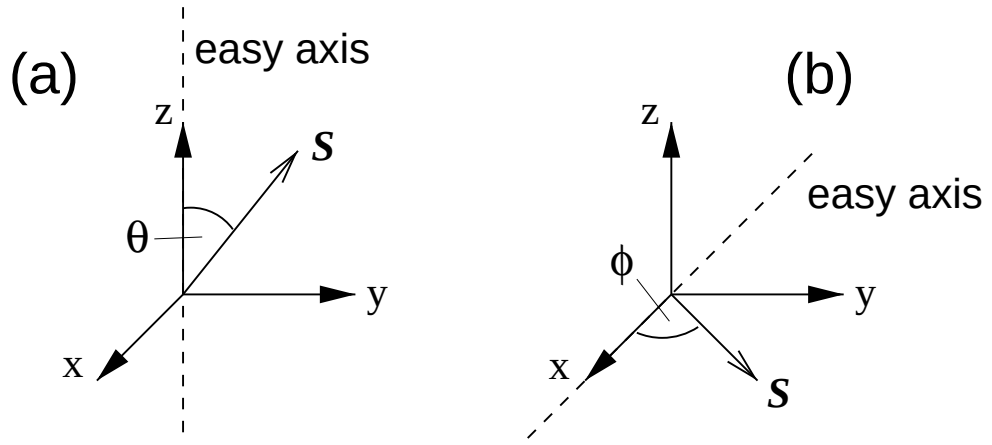

Figure 3.3: Two different cases for the island easy axes are assumed: (a) out-of-plane direction along the z axis, (b) in-plane direction along the x axis.

addition to the switching of single islands, magnetization reversals of island clusters are treated.

3.4.1 Angular-dependent magnetic energy of an island

We determine the magnetic energy of a single island of the interacting island system as function of the angle ϕ between its magnetization direction $\boldsymbol{S}_i$ and the positive direction of the easy axis. Two *stable* states for $\boldsymbol{S}_i$ along the easy axis are taken into account. We assume that during the rotation $S_i \rightarrow -S_i$ all other island moments of the system remain unchanged in the states $S_j = \pm 1$. Thus, deviations of the island magnetization directions from the easy axes are neglected, the island magnetizations remain always collinear. The external magnetic field $\boldsymbol{B}$ is always assumed to be parallel to the easy axes.

For the calculation of the dipole energy $E^i_{\rm dip}(\phi)$ of island i as resulting from Eq. (3.23) and the above mentioned assumptions, we distinguish two different cases for the easy axes, Fig. 3.3.

(1) Out-of-plane easy axes along the z axis: The dipole energy of the island as function of the polar angle θ between $\boldsymbol{S}_i$ and the $+\hat{\boldsymbol{z}}$-direction is obtained to be

$$E^i_{\rm dip}(\theta) = H^i_{\rm dip,1} \cos\theta \quad , \tag{3.25}$$

with the dipole field acting on island i

$$H^i_{\rm dip,1} = \mu_i \sum_j \mu_j \, S^z_j \left(\frac{x^2_{ij} + y^2_{ij}}{r^5_{ij}} \right) \quad . \tag{3.26}$$

(2) In-plane easy axes along the x axis: In this case, the dipole energy of the island as function of the azimuthal angle ϕ between $\boldsymbol{S}_i$ and the $+\hat{\boldsymbol{x}}$-direction is given by

$$E^i_{\rm dip}(\phi) = H^i_{\rm dip,2}\,\cos\phi - 3\,H^{*\,i}_{\rm dip,2}\,\sin\phi \quad , \tag{3.27}$$

with the dipole fields

$$H^i_{\rm dip,2} = \mu_i \sum_j \mu_j\, S^x_j \left(\frac{y^2_{ij} - 2\,x^2_{ij}}{r^5_{ij}}\right) \tag{3.28}$$

and

$$H^{*\,i}_{\rm dip,2} = \mu_i \sum_j \mu_j\, S^x_j \left(\frac{x_{ij}\; y_{ij}}{r^5_{ij}}\right) \quad . \tag{3.29}$$

In our calculations, we neglect the $\sin\phi$-term which will simplify the determination of the anisotropy energy barriers $\Delta E^{(1)}$.[8] For the energy differences $\Delta E^{(2)}$ between the stable states $S_i = \pm 1$, this term does not contribute.

If a particular geometry (1) or (2) is chosen, we will refer to the island spins S_i by use of the symbols S^z_i or S^x_i. We will use the common notation ϕ for both polar and azimuthal angles θ and ϕ.

In summary, the angular dependent magnetic energy of island i resulting from all terms of the micromagnetic model, Eq. (3.20), reads

$$E_i(\phi) = -H^i_{\rm ani}\;\cos^2\phi - \left(H^i_{\rm dw} - H^i_{\rm dip} + H^i_{\rm Z}\right)\;\cos\phi \quad , \tag{3.30}$$

with the anisotropy field

$$H^i_{\rm ani} = N_i\,K_i \quad , \tag{3.31}$$

the field resulting from the inter-island exchange coupling

$$H^i_{\rm dw} = \frac{1}{2}\sum_j L_{ij}\,\gamma_{ij}\,S_j \quad , \tag{3.32}$$

and the external field

$$H^i_{\rm Z} = \mu_i\,B \quad . \tag{3.33}$$

Analogously to Eq. (3.11) for the energy of a single island in an external field, we rewrite Eq. (3.30) to the more convenient expression

$$\epsilon_i(\phi) = \frac{E_i(\phi)}{H^i_{\rm ani}} = -\cos^2\phi - 2\,h^i_{\rm eff}\;\cos\phi \quad , \tag{3.34}$$

[8] This approximation is justified, since the ratio $3H^{*\,i}_{\rm dip,2}/H^i_{\rm dip,2}$ amounts in the average only to $\sim 20\,\%$, resulting in an underestimation of the energy barriers $\Delta E^{(1)}$ by $\sim 5\,\%$, if the dipole field is relevant.

with the reduced *effective* field resulting from all interaction terms

$$h^i_{\text{eff}} = \frac{H^i_{\text{dw}} - H^i_{\text{dip}} + H^i_{\text{Z}}}{2\,H^i_{\text{ani}}} \quad . \tag{3.35}$$

3.4.2 Rates of single-island magnetization flips

Analogously to the discussion of the magnetization reversal of an isolated single-domain particle in an external field (Sec. 3.2.1), we distinguish now two cases for the magnetization reversal and the corresponding flip rates of island i in respect to the *effective* interaction field, see also Fig. 3.2, p. 42:

1. $|h^i_{\text{eff}}| < 1$: During the forward or backward transition $S_i = \pm 1 \leftrightarrow S_i = \mp 1$ the island magnetization has to surmount the energy barrier resulting from the single-island anisotropy

$$\Delta E^{(1)}_i = H^i_{\text{ani}}\,(1 \pm h^i_{\text{eff}})^2 \quad . \tag{3.36}$$

   The rate of such a process is described by the Néel-Brown ansatz [112, 20, 21]

$$\Gamma^{(1)}_i = \Gamma_o \exp\left(-\Delta E^{(1)}_i / k_{\text{B}}T\right) \quad , \tag{3.37}$$

   with the attempt frequency $\Gamma_o \approx 1/\tau^{\text{c}}_{\text{pr}}$.

2. $|h^i_{\text{eff}}| \geq 1$: The two states $S_i = \pm 1$ refer to a maximum and a minimum. Here, the energy difference

$$\Delta E^{(2)}_i = \pm\, 4\, H^i_{\text{ani}}\, h^i_{\text{eff}} \tag{3.38}$$

   has to be surmounted during the reversal processes. We treat this case with the Metropolis-type rate [106, 92]

$$\Gamma^{(2)}_i = \begin{cases} \Gamma_o \exp\left(-\Delta E^{(2)}_i / k_{\text{B}}T\right) & , \ \Delta E^{(2)}_i > 0 \\ \Gamma_o & , \ \Delta E^{(2)}_i \leq 0 \end{cases} \quad , \tag{3.39}$$

   where an Arrhenius-type rate with the same attempt frequency Γ_o as given above is applied for the 'upward' thermal excitation, and the precession frequency Γ_o for the 'downward' transition to the lower energy state.

In Sec. 4.2.1, the single-spin-flip rates described by Eqs. (3.37) and (3.39) will be applied to MC simulations of the magnetic behavior of interacting island systems during growth.

3.4.3 Rates of island-cluster magnetization flips

The last part of this section is concerned with *coherent* magnetization reversals of island *clusters*, consisting of connected islands. The consideration of coherent island rotations is of eminent importance for efficient and more realistic calculations of the magnetic relaxation of a irregularly connected film using the MC method and allows for the calculation of the magnetic properties in the entire coverage range within the same model. The advantage of such a cluster MC method in contrast to conventional single-spin-flip algorithms, the construction procedure for the island clusters, and the application of the cluster-flip rates will be discussed in Sec. 4.2.2.

The flip rates of a spin cluster $\mathcal{C}_\nu = \{S_1, S_2, \ldots, S_\nu\}$ which we define as a set of connected islands are calculated in analogy to the previous subsection, as if the cluster forms a single large island. Note that the island moments within an island cluster need not to be parallel. Thus, the magnetic energy of this island cluster as function of angle ϕ between the island magnetization directions $\boldsymbol{S}_k$ and the easy axis is given by

$$\epsilon_\nu(\phi) = \frac{E_\nu(\phi)}{H^\nu_{\rm ani}} = -\cos^2\phi - 2\,h^\nu_{\rm eff}\cos\phi \quad . \tag{3.40}$$

The reduced *effective* field, acting on $\mathcal{C}_\nu$, reads

$$h^\nu_{\rm eff} = \frac{H^\nu_{\rm dw} - H^\nu_{\rm dip} + H^\nu_{\rm Z}}{2\,H^\nu_{\rm ani}} \quad , \tag{3.41}$$

where

$$H^\nu_{\rm ani} = \sum_k N_k\,K_k \quad , \tag{3.42}$$

and

$$H^\nu_{\rm dw} = \frac{1}{2}\sum_{kl} L_{kl}\,\gamma_{kl}\,S_k\,S_l \quad , \tag{3.43}$$

and

$$H^\nu_{\rm Z} = B\sum_k \mu_k\,S_k \tag{3.44}$$

are the corresponding fields, resulting from Eq. 3.20. The dipole field is given either by

$$H^\nu_{\rm dip,1} = \sum_{kl} \mu_k\,\mu_l\,S_k\,S_l\left(\frac{x^2_{kl}+y^2_{kl}}{r^5_{kl}}\right) \tag{3.45}$$

or by

$$H^\nu_{\rm dip,2} = \sum_{kl} \mu_k\,\mu_l\,S_k\,S_l\left(\frac{y^2_{kl}-2\,x^2_{kl}}{r^5_{kl}}\right) \quad , \tag{3.46}$$

depending on the chosen geometry for the local easy axis. The k-sums run over all spins *inside*, and the l-sums over all spins *outside* the spin cluster $\mathcal{C}_\nu$. We have made use of the condition $S_l = \pm 1$ during the rotation of the spin cluster. In case of an in-plane easy axis, we have again neglected the $\sin\phi$-term of Eq. (3.40), resulting from the dipole interaction.

Analogously to the previous subsection, for $|h^\nu_{\rm eff}| < 1$, the energy barriers

$$\Delta E^{(1)}_\nu = H^\nu_{\rm ani}\,(1 \pm h^\nu_{\rm eff})^2 \tag{3.47}$$

have to be surmounted. For this, the Arrhenius-type cluster-flip rate $\Gamma^{(1)}_\nu$ given by Eq. (3.37) is applied. For $|h^{\rm eff}_\nu| \geq 1$, the cluster-flip rate $\Gamma^{(2)}_\nu$ is calculated by use of the Metropolis-type rate, Eq. (3.39), considering the energy difference

$$\Delta E^{(2)}_\nu = \pm\, 4\, H^\nu_{\rm ani}\, h^\nu_{\rm eff} \quad . \tag{3.48}$$

In Sec. 4.2.2, these cluster-flip rates will be applied to cluster MC simulations of the magnetic behavior of *irregularly* connected island spin systems during growth. We will see that for such systems single-spin-flips are not suited.